

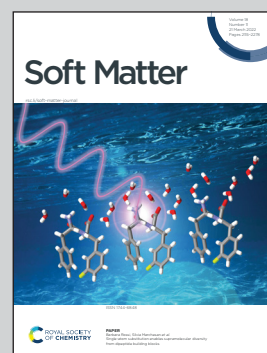


Highlighting research from Marie Tani and Rei Kurita,  
Department of Physics, Tokyo Metropolitan University,  
Japan.

Pinch-off from a foam droplet in a Hele-Shaw cell

A foamy droplet put on a vertical wall sometimes loses its solution due to a liquid pinch-off from the bottom. The onset of the phenomenon is explained by a simple model.

As featured in:



See Marie Tani and Rei Kurita,  
*Soft Matter*, 2022, **18**, 2137.



Cite this: *Soft Matter*, 2022, 18, 2137

Received 2nd September 2021,  
Accepted 7th February 2022

DOI: 10.1039/d1sm01268a

[rsc.li/soft-matter-journal](http://rsc.li/soft-matter-journal)

# Pinch-off from a foam droplet in a Hele-Shaw cell†

Marie Tani \* and Rei Kurita

Placing some foam on a vertical surface is a ubiquitous situation, for example, such as in shaving and wall cleaning in daily life, and in egg-laying or making foam nests for some animals or insects in nature. In such a situation, one may prefer that the foam remains in the initial position. Moreover, losing solution via liquid pinch-off from the bottom of the foam is undesirable. To address the pinching off condition and mechanism, we conducted a model experiment: we confined an amount of foam in a Hele-Shaw cell. Two sliding down modes, both with and without liquid pinch-off, were observed under gravity. We fabricated morphology phase diagrams, and theoretically clarified the onset of liquid pinch-off from a foamy droplet.

## 1 Introduction

A foam is a jammed state where gas bubbles are compacted in a surfactant solution.<sup>1,2</sup> Although a foam is composed only of fluids, it shows both solid-like and liquid-like behavior. Its mechanical properties, such as elasticity, viscosity and yield stress, depend strongly on the liquid fraction.<sup>3–10</sup> Using these complexities, foams are ubiquitously applied in our everyday life, as in foods, detergents, cosmetic products and pharmaceuticals.

In nature, some animals and insects take advantage of foams. For example, some frogs or fishes put their eggs in foam nests.<sup>11–13</sup> The nymphs of froghoppers, which are commonly named spittlebugs, live in foamy nests put on plants for protection and thermal and moisture control.<sup>14,15</sup> We also place some amounts of foam on our faces during shaving, or on vertical walls when cleaning them. In such a situation, one may prefer that the foam remains in its initial state and in its initial position. A worse case may be when a foamy droplet loses some of its solution due to a liquid pinch-off from the bottom of the droplet, as seen in Fig. 1(a). This seems to be caused by the aggregation of the liquid due to drainage in the foam. However, the condition and the mechanism of this phenomenon are unclear. The foam will be drier if the pinch-off occurs since a large amount of liquid can be lost. Furthermore, the decrease in the liquid fraction can drastically decrease the stability of the foam since dry foam is more likely to collapse than wet foam.<sup>1,2,6,8,10</sup> Thus, to clarify the condition of the liquid pinch-off from a foamy drop is an important issue as well as a fundamental problem.

The pinch-off condition was first reported by Tate in 1864 for a liquid droplet hanging from a nozzle.<sup>16,17</sup> The dynamics of the pinch-off have received great interest over the past decades due to the issues of topology, singularity or self-similarity,<sup>18–22</sup> not only for Newtonian fluids but also for complex fluids.<sup>23–26</sup> Liquid or gas pinch-off is also important in the context of microfluidics as droplets and bubbles are formed by pinch-off in T-junction or flow-focusing devices.<sup>27,28</sup> Although there have been some studies on pinching off in foams, these reports have been limited to cases where the foams themselves pinch off as complex fluids.<sup>24,25</sup> Thus, the condition and mechanism of liquid pinching-off from a foamy droplet are not yet clear.

In this paper, we describe when liquid pinches off from a foamy droplet. We carried out a model experiment: we confined an amount of foam in a Hele-Shaw cell and tilted the cell as shown in Fig. 1(b). Through gravitational force, the foamy droplet starts to fall down in the cell. In some cases, liquid aggregating at the bottom of the foam pinches off with the formation of a liquid thread (“pinch-off”), although there are some cases where the entire foam slides down (“no pinch-off”) as shown in Fig. 1(c1) and (c2), respectively (movies are also available as ESI†). We made morphology phase diagrams and theoretically estimated the lower border of the two modes. We found that adopting Tate’s law explains well the critical mass of drained liquid above which the liquid pinches off. Furthermore, we discuss the problem in three-dimensional cases.

## 2 Experimental methods

The experimental setup is shown in Fig. 1(b). We confined an amount of foam in a Hele-Shaw cell. For the foam solution, we used a 20 wt% dilution of a commercial dish soap (Charmy, Lion Co., Japan). The concentration is sufficiently higher than

Department of Physics, Tokyo Metropolitan University, Tokyo, Japan.

E-mail: [mtani@tmu.ac.jp](mailto:mtani@tmu.ac.jp)

† Electronic supplementary information (ESI) available. See DOI: 10.1039/d1sm01268a



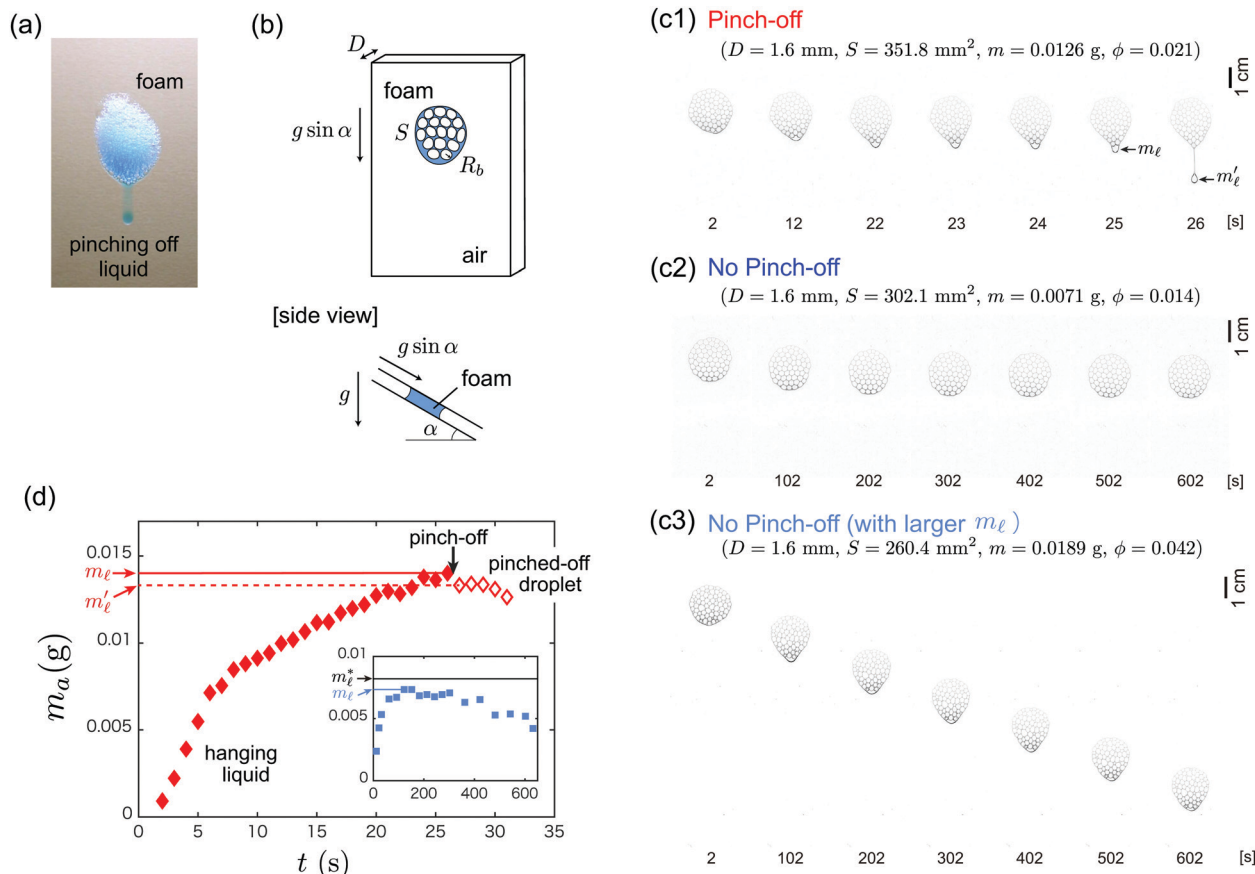


**Fig. 1** (a) A typical situation in everyday life: liquid pinches off from the bottom of a foamy droplet placed on a vertical wall. (b) Experimental setup and (c) series of pictures observed in our experiments: (c1) "pinch-off" (P) and (c2) "no pinch-off" (NP) modes, and (c3) NP modes with larger  $m_l$ . The time indicated below each picture is the elapsed time since the cell was tilted.  $D$  is the inner gap of the cell, and  $S$ ,  $m$  and  $\phi$  are the surface area, mass and liquid fraction of the foamy droplet, respectively. Movies of each pattern are also available. (d) Aggregating mass  $m_a$  at the bottom of the foamy droplet (solid symbols) and mass of pinched-off droplet (open symbols) as a function of the elapsed time for the P mode (main) and NP mode with larger  $m_l$  (inset). Here,  $m_l$  and  $m'_l$  for the P modes are defined as  $m_a$  just before and just after liquid pinch off, respectively.  $m_l$  for the NP mode is defined as the maximum value of  $m_a$ .

the critical micelle concentration ( $\approx 0.3$  wt%). The surface tension of the solution was measured as  $\gamma = 25 \pm 2$  mN m<sup>-1</sup> using a Denuce' surface tension tester D (Itoh, Japan). The density of the solution was estimated from the mass of a certain volume of the solution as  $\rho = 1.07 \pm 0.02$  g cm<sup>-3</sup>. Then, foam was made by injecting air into the solution. We injected air into the solution in a beaker using a syringe with a needle of inner diameter 0.41 mm (NN-2238S, Terumo, Japan). The injection flow rate was set to 10 ml min<sup>-1</sup> using a syringe pump (Fusion 200, Chemyx Inc., USA). From this, we obtained air bubbles whose radii are about 1 mm.

The Hele-Shaw cell is made of acrylic plates. We confirmed that the solution wets the plate well; the contact angle of a settled drop on a horizontal acrylic plate was measured to be about 10 degrees or less for the equilibrium value. The cell width and height are 60–80 mm and 200–300 mm, respectively. The inner gap  $D$  is set to 0.5, 0.8, and 1.6 mm so that  $D/2$  is smaller than the capillary length  $\kappa^{-1} = \sqrt{\gamma/\rho g} = 1.5$  mm, where  $g = 9.8$  m s<sup>-2</sup> is the gravitational acceleration. Therefore,

the solution can remain in contact with both cell plates even if the liquid aggregates and pinches off.

We then put an amount of foam on a cell plate, and put the other plate on the foam after inserting a spacer whose thickness corresponds to the gap length  $D$ . As a result, we obtained a circular foam droplet where one layer of bubbles is confined. The radius of the confined bubbles in the cell  $R_b$  was estimated from all bubbles in the foam droplet and taking an average of more than ten samples for each value of the gap  $D$ . Then, we obtained the mean values and standard deviations as follows:  $1.1 \pm 0.1$ ,  $1.8 \pm 0.1$ , and  $2.0 \pm 0.1$  mm for the cell thickness  $D = 1.6$ , 0.8, and 0.5 mm, respectively.

Then, we tilted the cell to observe how the foam droplet behaves under gravity. We set the tilting angle  $\alpha$  as  $\alpha = 30$ , 45, and 90° to change the effective gravity  $\tilde{g} = g \sin \alpha$ . We then measured the surface area of the foamy droplet  $S$  on a picture such as that shown in Fig. 1(c). After each experiment, the foam and the liquid wetting the cell walls were wiped away carefully using soft tissues to calculate the mass of liquid  $m$  included in



the foam. As a result, we obtained the liquid fraction  $\phi$  as  $\phi = m/\rho SD$ . The uncertainty in the measurements of the mass of the foamy droplet is about 0.0005 g.

### 3 Results and discussion

As the cell is tilted, the foamy droplet starts to slide down inside the cell as shown in Fig. 1(c). In some cases, the liquid aggregating at the bottom of the foamy droplet pinched off (“pinch-off” (P) mode), making a liquid thread as shown in Fig. 1(c1). By contrast, sometimes the liquid does not pinch off and the entire foam droplet slides down (“no pinch-off” (NP) mode) as shown in Fig. 1(c2). The aggregation of the liquid was also confirmed in Fig. 1(d), where the aggregating liquid mass  $m_a$  is plotted as a function of the elapsed time. Here,  $m_a$  is estimated as  $m_a = \rho S_a D$  where  $S_a$  is the measured area of the accumulating liquid at the bottom of the foam in pictures shown in Fig. 1(c1).

To clarify the condition determining the falling down patterns, we made a morphology phase diagram. Fig. 2(a) shows

observed falling patterns as a function of the area of the foam droplet  $S$ , and the liquid mass in the foam  $m$ , for the case where  $D = 1.6$  mm and  $\alpha = 90^\circ$ . The “pinch-off” (P) mode (full circles) is seen in the larger  $m$  region, and the “no pinch-off” (NP) mode (open squares) is seen in the smaller  $m$  or smaller  $S$  region. The color of each symbol represents the liquid fraction  $\phi$  of the foam. We note that it is difficult to approach the larger  $S$  and smaller  $m$  regions as foam is too dry to be maintained. The diagram implies the existence of an onset below which the liquid does not pinch off from a foamy droplet.

We shall begin theoretical arguments for the case where a hanging liquid droplet pinches off from a rigid cylindrical nozzle. It may be easily imagined that the liquid pinches off as the self-weight of the liquid droplet exceeds the capillary force. Thus, liquid pinches off if:

$$\Omega_\ell > \frac{2\pi R\gamma}{\rho g}, \quad (1)$$

where  $\Omega_\ell$  is the volume of the hanging liquid and  $R$  is the nozzle radius. This is known as Tate's law.<sup>16,17</sup>

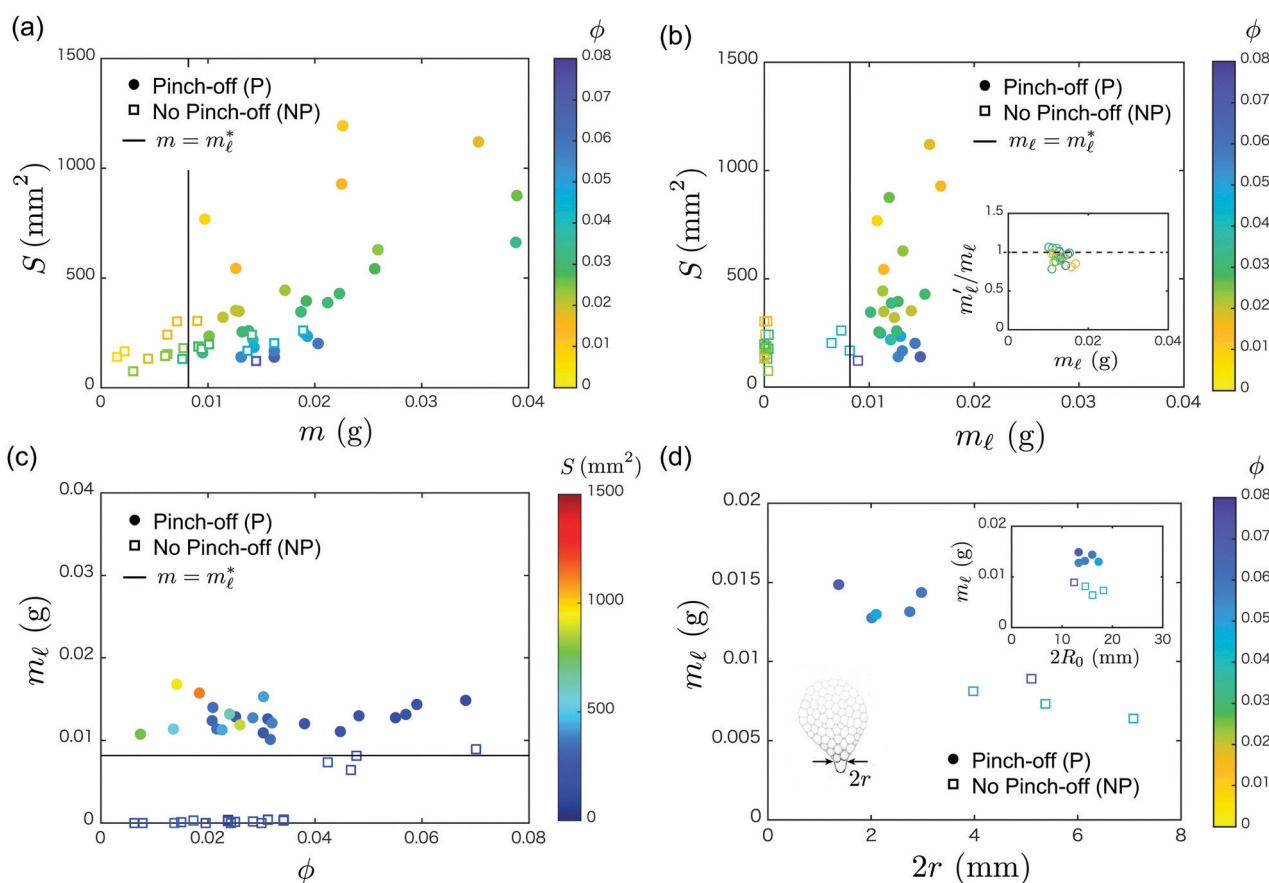


**Fig. 2** (a) and (b) Phase diagrams of observed falling down patterns for  $D = 1.6$  mm and  $\alpha = 90^\circ$ . The patterns are mapped as a function of (a) the area of the droplet  $S$  and the liquid mass included in the foam  $m$ , and (b)  $S$  and the estimated liquid mass accumulating at the bottom of the foam  $m_\ell$ . Filled circles and open squares denote the “pinch-off” (P) and “no pinch-off” (NP) modes, respectively. The color of each symbol represents the liquid fraction  $\phi$  of the foam. Black solid lines are the predicted lower border of the P mode, i.e.,  $m = m_\ell^*$  and  $m_\ell = m_\ell^*$ , respectively. The inset shows the ratio of the estimated liquid mass after and before pinch-off,  $m'_\ell/m_\ell$ , as a function of  $m_\ell$ . (c)  $m_\ell$  as a function of  $\phi$  where the colors indicate the  $S$  value. (d)  $m_\ell$  as a function of  $2r$  (main) and  $2R_0$  (inset). The definition of  $2r$  is seen in the plot.  $R_0$  is the initial radius of the foamy droplet, which is calculated as  $R_0 = \sqrt{(S/\pi)}$ . The colors represent the values of  $\phi$ .





Then, let us consider a case where a liquid droplet is confined between two plates. If the liquid wets the plates well, thin liquid films remain on the plates after the droplet deforms. Then, if the volume of these liquid films is negligible, the capillary force can be estimated as  $2D\gamma$ , where  $D$  is the gap between the plates.<sup>29,30</sup> As a result, we obtain the pinch-off condition as  $\Omega_\ell > 2D\gamma/(\rho g)$ .

We now move on to the foamy droplet case in a Hele-Shaw cell. As a foam is placed under gravity, liquid is drained in the foam and aggregates at the bottom of the foam droplet. It follows that the upper part of the foamy droplet becomes drier. Since viscous friction in the thin liquid films between the walls and the air bubbles is larger compared with that in the bulk liquid,<sup>31–33</sup> the upper part of the foamy droplet moves more slowly compared with the liquid part. As a result, the aggregating liquid hangs from the foam part. Therefore, adapting Tate's law as the pinch-off condition seems to be reasonable if liquid is drained well from the foam. If we indicate the liquid mass aggregating at the bottom of the foam  $m_\ell = \rho\Omega_\ell$ , we obtain

$$m_\ell > m_\ell^* = \frac{2D\gamma}{g \sin \alpha}, \quad (2)$$

where  $\alpha$  is the tilting angle of the cell. If most liquid in the foamy droplet aggregates at the bottom of the foam due to foam drainage, i.e.,  $\Omega_\ell \simeq \Omega_\ell^{\text{foam}}$  or  $m_\ell \simeq m$ , where  $\Omega_\ell^{\text{foam}}$  and  $m$  are the volume and mass of liquid included in the foamy droplet, respectively, the pinch-off condition is written as  $m > m_\ell^*$ .

The value  $m_\ell^*$  is 0.0082 g for  $D = 1.6$  mm and the tilting angle  $\alpha = 90^\circ$ , which is indicated by the solid line in Fig. 2(a). Fig. 2(b) shows a similar phase diagram, although the aggregating liquid mass  $m_\ell$  is used as the horizontal axis instead of using the total liquid mass  $m$ . Here,  $m_\ell$  is defined as  $m_a$  just before the liquid pinches off for the P mode as indicated in Fig. 1(c1) and (d). For the NP mode,  $m_a$  initially increases, and then decreases as seen in the inset of Fig. 1(d). This decrease seems to be because some amount of liquid in the foamy droplet remains at the wall. Thus, we defined  $m_\ell$  as the maximum value of  $m_a$  for the NP mode. We found that the predicted critical mass  $m_\ell^*$  more clearly separates the NP and P modes in Fig. 2(b). However, the NP mode can also be observed in the region  $m > m_\ell^*$ , as seen in Fig. 2(a). Therefore, the aggregating liquid mass  $m_\ell$  seems to be more important than the total liquid mass  $m$  in the foam.

To understand what happens in the NP mode where  $m > m_\ell^*$ , we first discuss whether  $m_\ell$  is determined by foam drainage. It is known that liquid comes out from the foam due to foam drainage, and that the liquid fraction becomes about 0.16 at the border between the pure liquid and the foam in a two-dimensional system. However, it is not applied in a quite dry foam or a small amount of foam, where the total amount of liquid is small.<sup>2</sup> Indeed, this is seen in our experiment: Fig. 2(c) shows that  $m_\ell$  is almost zero for smaller  $S$  and smaller  $\phi$  or smaller  $m$ , and, in fact, NP modes observed in the  $m > m_\ell^*$  region have small  $S$  as seen in Fig. 2(a). Furthermore, we plot  $m_\ell$  as a function of some geometrical values ( $2r$  and  $2R_0$ ) in Fig. 2(d). Here,  $2r$  is the “nozzle” width as seen in the plot at

the time when  $m_\ell$  is defined.  $R_0$  is the initial radius of the foamy droplet, which is calculated from the surface area  $S$  of the foamy droplet;  $R_0 = \sqrt{S/\pi}$ . We found that  $m_\ell$  is larger for smaller “nozzle” width  $2r$ , although it is independent of the initial size of the foamy droplet  $R_0$ . By following the drainage equations,<sup>1,2,34</sup> foam dries with a height from the interface between the bubbles and pure solution. Thus, more liquid is drained and larger  $m_\ell$  is realized for a foamy droplet with larger vertical length. However,  $m_\ell$  does not depend on the initial size of the foamy droplet  $R_0$ . On the other hand, for the lower region of the foam droplet, plateau borders (PBs) have larger cross-sections since the liquid fraction is large. In addition, it is known that the amount of liquid in “horizontal” PBs (i.e., PBs perpendicular to the walls) is larger than that in “wall” PBs (i.e., PBs parallel to the walls) in a quasi-two dimensional foam.<sup>35</sup> The number of such wider horizontal PBs decreases for smaller  $r$ . As a result,  $m_\ell$  becomes larger for smaller  $r$ . However, we still have questions on how foamy droplets, which are initially circular, become narrower shapes.

To address this point, we shall review the sequences of pictures in Fig. 1(c). In the P mode, the foamy droplet elongates with the rearrangement of air bubbles. By contrast, in NP mode, the foamy droplet retains its shape and no rearrangement of air bubbles occurs after 100 s, even if it has a larger  $m_\ell$  as seen in Fig. 1(c3). In addition, some amount of liquid seems to be trapped between the lower air bubbles. It seems that the liquid that remains in horizontal PBs can flow out drastically if some rearrangements of the air bubbles occur. Then, the occurrence of the rearrangement may depend on the relative velocity of the hanging liquid part to the foamy area. However, the details of the dynamics and the mechanism of liquid aggregation are not yet clear, and more precise work is needed in the future. Furthermore, it may be worth noting that the dynamics of foam drainage in a finite system and in a moving foam with lubrication films, which causes the loss of an amount of liquid in the foam, can be different from liquid drainage in an infinite bulk of the foam. We also note that there is a point of the NP mode in the area of  $m_\ell > m_\ell^*$  in Fig. 2. For this point, although  $m_\ell$  (the maximum of  $m_a$ ) is larger than  $m_\ell^*$ , it then decreases and becomes less than  $m_\ell^*$  before a liquid pinch-off happens. We emphasize that our prediction still explains well the experimental results such as the onset of the P mode.

For the P mode, we also estimated the mass of aggregating liquid at the bottom of the foam just before pinch-off  $m_\ell$  and that after pinch-off  $m'_\ell$ , as shown in the inset of Fig. 2(b). We found that more than 80% of the accumulating liquid pinches off, which is different from the ordinary three-dimensional liquid case known as Tate's law,<sup>16</sup> where only about 60% of the mass of the pendant liquid becomes a droplet.<sup>17</sup> This may be because the pinched-off liquid falls down and makes a liquid thread as shown in Fig. 1(c1) differently from the three-dimensional inviscid liquid case. It seems that this thread can lead to more liquid loss of the foam even after the liquid has pinched off. It may be worth mentioning that a foam can lose the most amount of liquid if the aggregating liquid pinches off.



Furthermore, we examined the prediction with our experimental results using a different inner cell thickness  $D$  and tilting angle  $\alpha$ . The observed patterns are mapped as a function of the area of the foamy droplet  $S$  and the liquid mass accumulating at the bottom of the foamy droplet  $m_\ell$  normalized by the threshold value  $m_\ell^*$  as shown in Fig. 3(a). As seen here, the prediction indicated as the solid line describes well the onset of the P mode.

The value that best characterizes a foam may be the liquid fraction  $\phi$  rather than the liquid mass  $m$ . Thus, we shall rewrite the threshold. As the volume of the liquid in a foam is written as  $\Omega_\ell^{\text{foam}} = \phi S D$  where  $\phi$  is liquid fraction, we obtain

$$S > S^* = \frac{2\gamma}{\rho g \sin \alpha} \frac{1}{\phi}. \quad (3)$$

By noting  $S_0^* = 2\gamma/(\rho g \sin \alpha)$ , the condition is written as  $S > S_0^*/\phi$ . This is tested in Fig. 3(b), and we can see that it also explains our experimental results well.

The pinch-off time mainly depends on the time for liquid to accumulate at the bottom of the foam, *i.e.*, the drainage dynamics. For the same cell thickness  $D$  (thus the same size of air bubbles  $R_b$ ), the pinch-off time is larger for a smaller

liquid mass. However, the typical pinch-off times are similar for different cell thickness  $D$  and similar liquid mass  $m$ . It seems that  $D$  is related to  $m_\ell^*$ , but not so much to the drainage time scale. This is consistent with the fact that most drainage occurs on the walls in a foam in a Hele-Shaw cell.<sup>35</sup>

For further discussion, we carried out an additional experiment with a foam where multilayers of tiny air bubbles are placed between the cell plates, for  $D = 1.6$  mm and  $\alpha = 90^\circ$ . The foam was made using a commercial pump for making foams of hand-soap solution. The typical radius of bubbles is  $0.25 \pm 0.06$  mm although some bubbles are much larger because of coarsening. In fact, liquid drainage takes much time, and the time it takes for the liquid to pinch off is about one order larger compared with that in the previous cases. This is reasonable because the drainage is slower for the smaller bubble size in the foam.<sup>1,2</sup> However, two falling down modes are still observed if we wait for long enough, and these are well explained in the same morphology diagram as indicated by the star symbols in Fig. 3.

Finally, we examined a three-dimensional case, namely the problem that we were originally interested in. We placed an amount of foam on a vertical acrylic plate. As shown in Fig. 4, two modes are observed, similar to the quasi-two-dimensional cases. The pictures in the plot are typical snapshots of each mode, where some blue dye was added to the solution to make the samples easy to see, although the dye was not added for obtaining the experiment data. It seems to be natural to take the capillary length  $\kappa^{-1}$  as the typical length scale in this case, since the hanging liquid droplet has a three-dimensional shape. In fact, the width of the footprint of the pendant droplet  $\ell$  is 3.1 mm, which is approximately the same as  $2\kappa^{-1}$ . This

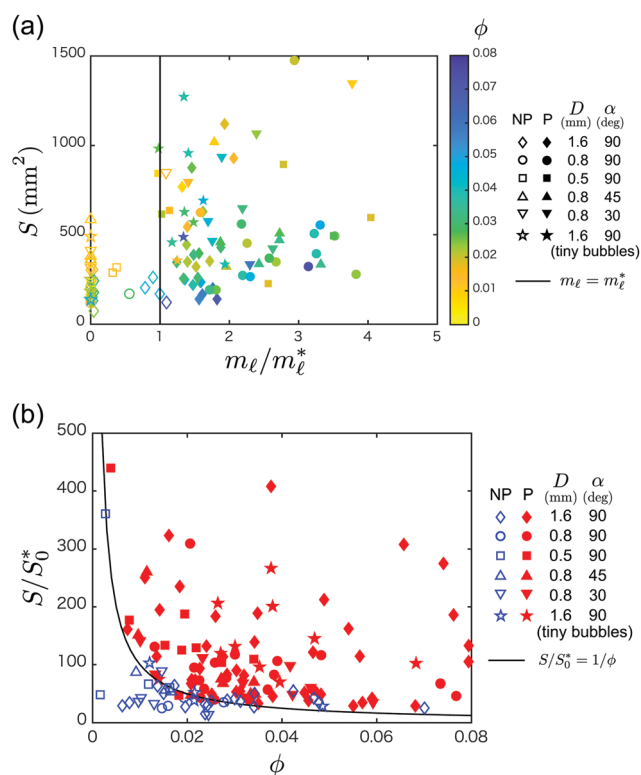


**Fig. 3** Morphology phase diagrams where the observed patterns are mapped as a function of (a) the surface area of the foam  $S$  and the normalized liquid mass  $m_\ell/m_\ell^*$ , and (b) the normalized area  $S/S_0^*$  and the liquid fraction  $\phi$ , respectively. Open and solid symbols indicate the “no pinch-off” (NP) and “pinch-off” (P) patterns, respectively. The color of each symbol in (a) represents the liquid fraction  $\phi$  of the foam. Black solid lines are the predicted threshold of the pinch-off:  $m_\ell = m_\ell^*$  and  $S/S_0^* = 1/\phi$ , respectively. Some experimental results where multilayers of tiny bubbles were put into the cell are added as star symbols.

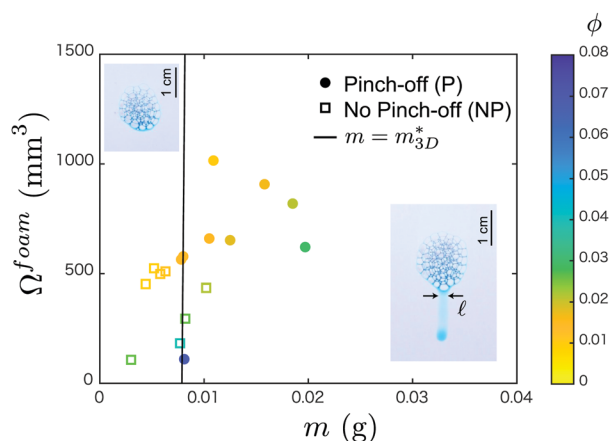


**Fig. 4** Morphology phase diagram in the three-dimensional case where an amount of foam was put on a vertical plate ( $\alpha = 90^\circ$ ). The observed falling down patterns are mapped as a function of the volume of the foamy droplet  $\Omega^{\text{foam}}$  and the liquid mass  $m$ . Filled circles and open squares denote the “pinch-off” (P) and “no pinch-off” (NP) modes, respectively, and the colors represent the liquid fraction  $\phi$  for each foam. The black line is the predicted onset of the P mode. The inset pictures in the plot are typical snapshots of each mode, where some blue dye was added to the solution to make things easier to see, although the dye was not added for obtaining the experiment data.

leads to the capillary force  $2\kappa^{-1}\gamma$  and the pinch-off condition:  $m > m_{3D}^* = 2\kappa^{-1}\gamma/(g\sin\alpha)$ . Here,  $m_{3D}^*$  is estimated to be about 0.0079 g. The prediction again explains the onset of pinch-off well, as indicated by the solid line in the plot.

## 4 Conclusion

We focused on a ubiquitous phenomenon of liquid pinching off from a foamy droplet placed on a vertical wall, and carried out model experiments. We confined an amount of aqueous foam in a Hele-Shaw cell, set the cell to a tilting angle, and observed the sliding down behavior of the foamy droplet. We found two falling down modes: the “pinch-off” mode, where liquid that drains from the foam aggregates at the bottom of the foamy droplet and pinches off; and the “no pinch-off” mode, where the entire foamy droplet falls down without liquid pinching off. We described the threshold of pinch-off by adapting Tate’s law.<sup>16</sup> The prediction explains the onset of pinch-off mode well in the morphology phase diagrams. Furthermore, we succeeded in determining the pinch-off onset in the original three-dimensional case. Our results predict the critical mass of drained liquid above which pinch-off may occur in a finite amount of foam placed on a vertical wall; a foam with a lower liquid mass does not cause the liquid to pinch-off, and a foam composed of tiny air bubbles indirectly suppresses it by slowing the drainage rate of the foam.

## Author contributions

M.T. conceived the project, performed the experiments and analyzed the data. M.T. and R.K. considered the mechanism of liquid pinch-off. M.T. wrote the manuscript.

## Conflicts of interest

There are no conflicts to declare.

## Acknowledgements

M.T. and R.K. were supported by JSPS KAKENHI (20K14431, 17H02945 and 20H01874).

## References

- 1 D. L. Weaire and S. Hutzler, *The physics of foams*, Oxford University Press, 2001.
- 2 I. Cantat, S. Cohen-Addad, F. Elias, F. Graner, R. Höhler, O. Pitois, F. Rouyer and A. Saint-Jalmes, *Foams: structure and dynamics*, OUP Oxford, 2013.
- 3 A. M. Kraynik, *Annu. Rev. Fluid Mech.*, 1988, **20**, 325–357.
- 4 G. Debregeas, H. Tabuteau and J.-M. Di Meglio, *Phys. Rev. Lett.*, 2001, **87**, 178305.
- 5 R. Höhler and S. Cohen-Addad, *J. Phys.: Condens. Matter*, 2005, **17**, R1041.
- 6 A.-L. Biance, A. Delbos and O. Pitois, *Phys. Rev. Lett.*, 2011, **106**, 068301.
- 7 S. Cohen-Addad, R. Höhler and O. Pitois, *Annu. Rev. Fluid Mech.*, 2013, **45**, 241–267.
- 8 Y. Furuta, N. Oikawa and R. Kurita, *Sci. Rep.*, 2016, **6**, 1–8.
- 9 N. Yanagisawa and R. Kurita, *Sci. Rep.*, 2019, **9**, 1–9.
- 10 N. Yanagisawa, M. Tani and R. Kurita, *Soft Matter*, 2021, **17**, 1738–1745.
- 11 R. I. Fleming, C. D. Mackenzie, A. Cooper and M. W. Kennedy, *Proc. R. Soc. London, Ser. B*, 2009, **276**, 1787–1795.
- 12 D. Andrade and A. S. Abe, *J. Fish Biol.*, 1997, **50**, 665–667.
- 13 A. Cooper and M. W. Kennedy, *Biophys. Chem.*, 2010, **151**, 96–104.
- 14 E. Keskinen and V. B. Meyer-Rochow, *Arthropod Struct. Dev.*, 2004, **33**, 405–417.
- 15 M. Tonelli, G. Gomes, W. D. Silva, N. T. Magri, D. M. Vieira, C. L. Aguiar and J. M. S. Bento, *Sci. Rep.*, 2018, **8**, 1–6.
- 16 T. Tate, *London, Edinburgh Dublin Philos. Mag. J. Sci.*, 1864, **27**, 176–180.
- 17 P.-G. De Gennes, F. Brochard-Wyart and D. Quéré, *Capillarity and wetting phenomena: drops, bubbles, pearls, waves*, Springer Science & Business Media, 2013.
- 18 J. Eggers, *Phys. Rev. Lett.*, 1993, **71**, 3458.
- 19 M. P. Brenner, X. Shi and S. R. Nagel, *Phys. Rev. Lett.*, 1994, **73**, 3391.
- 20 P. Constantin, T. F. Dupont, R. E. Goldstein, L. P. Kadanoff, M. J. Shelley and S.-M. Zhou, *Phys. Rev. E: Stat. Phys., Plasmas, Fluids, Relat. Interdiscip. Top.*, 1993, **47**, 4169.
- 21 R. E. Goldstein, A. I. Pesci and M. J. Shelley, *Phys. Rev. Lett.*, 1993, **70**, 3043.
- 22 H.-G. Lee, J. Lowengrub and J. Goodman, *Phys. Fluids*, 2002, **14**, 492–513.
- 23 P. Coussot and F. Gaulard, *Phys. Rev. E: Stat., Nonlinear, Soft Matter Phys.*, 2005, **72**, 031409.
- 24 F. Huisman, S. Friedman and P. Taborek, *Soft Matter*, 2012, **8**, 6767–6774.
- 25 C.-C. Kuo and M. Dennin, *Phys. Rev. E: Stat., Nonlinear, Soft Matter Phys.*, 2013, **87**, 052308.
- 26 V. Thiévenaz, S. Rajesh and A. Sauret, *Soft Matter*, 2021, **17**, 6202–6211.
- 27 R. Dangla, S. Lee and C. N. Baroud, *Phys. Rev. Lett.*, 2011, **107**, 124501.
- 28 G. Amselem, P. Brun, F. Gallaire and C. N. Baroud, *Phys. Rev. Appl.*, 2015, **3**, 054006.
- 29 J. Bico and D. Quéré, *J. Fluid Mech.*, 2002, **467**, 101–127.
- 30 M. Tani, R. Kawano, K. Kamiya and K. Okumura, *Sci. Rep.*, 2015, **5**, 1–14.
- 31 A. Eri and K. Okumura, *Soft Matter*, 2011, **7**, 5648–5653.
- 32 M. Yahashi, N. Kimoto and K. Okumura, *Sci. Rep.*, 2016, **6**, 1–8.
- 33 L. Keiser, K. Jaafar, J. Bico and E. Reyssat, *J. Fluid Mech.*, 2018, **845**, 245–262.
- 34 A. Tani and M. Tani, *J. Math. Anal. Appl.*, 2021, **504**, 125573.
- 35 M. Tong, K. Cole and S. Neethling, *Colloids Surf., A*, 2011, **382**, 42–49.

